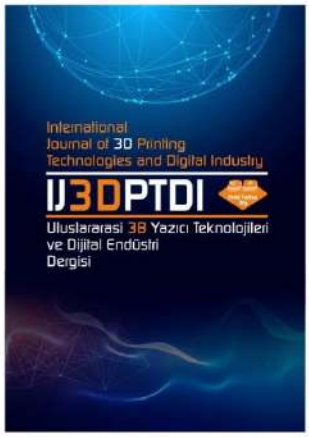

ULUSLARARASI 3B YAZICI TEKNOLOJİLERİ
VE DİJİTAL ENDÜSTRİ DERGİSİ

INTERNATIONAL JOURNAL OF 3D PRINTING
TECHNOLOGIES AND DIGITAL INDUSTRY

ISSN:2602-3350 (Online)

URL: https://dergipark.org.tr/ij3dptdi

MANUFACTURING AND CHARACTERIZATION OF WAAM-BASED BIMETALLIC CUTTING EQUIPMENT

Yazarlar (Authors):Uğur Gürol*,Savaş Dilibal,Batuhan Turgut,Hakan Baykal ,Hülya Kümek,Mustafa Koçak

Bu makaleye şu şekilde atıfta bulunabilirsiniz (To cite to this article): *Gürol U., Dilibal S., Turgut B., Baykal H., Kümek H., Koçak M., "Manufacturing and Characterization of Waam-Based Bimetallic Cutting Equipment" Int. J. of 3D Printing Tech. Dig. Ind., 6(3): 548-555, (2022).*

DOI: 10.46519/ij3dptdi.1210836

Araştırma Makale/ Research Article

Erişim Linki: (To link to this article): https://dergipark.org.tr/en/pub/ij3dptdi/archive

MANUFACTURING AND CHARACTERIZATION OF WAAM-BASED BIMETALLIC CUTTING EQUIPMENT

Uğur Gürol[a,b]*,Savaş Dilibal[c,d],Batuhan Turgut[e],Hakan Baykal[e],Hülya Kümek[e],Mustafa Koçak[f]

[a]İstanbul Gedik University, Metallurgical and Materials Engineering Department, İstanbul, TURKEY
[b]İstanbul Gedik University, Welding Technologies Application and Research Center, İstanbul, TURKEY
[c]İstanbul Gedik University, Mechatronics Engineering Department, İstanbul, TURKEY
[d]İstanbul Gedik University, Robot Technologies Application and Research Center, İstanbul, TURKEY
[e]Gedik Welding Inc., Research and Development Center, İstanbul, TURKEY
[f]İstanbul Gedik University, Mechanical Engineering Department, İstanbul, TURKEY

* *Corresponding Author: ugur.gurol@yahoo.com*

(**Received:** 28.11.2022; **Revised:** 05.12.2022; **Accepted:**29.12.2022)

ABSTRACT

Wire-arc additive manufacturing (WAAM) is a promising method to produce many functional components in different industries. In this method, the welding wires from the feedstock are melted by arc discharge and deposited layer by layer. Other welding wires having different chemical compositions can also be added to the top of the previously deposited layer by replacing the feed wire from the stock to produce bimetallic components. This study investigated the feasibility of using robotic wire arc additive manufacturing technology to produce a bimetallic cutting equipment. The bimetallic cutting equipment was produced by depositing MSG 6 GZ-60 hard-facing welding wire on top of the austenitic stainless-steel wall produced with ER 316LSi solid wire. The cutting-based equipment requires an increased abrasion resistance with the combination of ductility to provide adequate equipment life and performance. Thus, detailed microstructural analysis and hardness tests were conducted to understand the general microstructural characteristic of the manufactured cutting equipment, including interfaces between two different materials.

Keywords: Metal Additive Manufacturing, Wire Arc Additive Manufacturing, Cutting Equipment, Bimetallic Structure.

1. INTRODUCTION

It is well-known that metal additive manufacturing technologies provide tailor-based structures to produce various 3D components in the industry [1]. The joining of two metallic materials with different mechanical properties can provide many functionally graded materials (FGM). Bimetallic additively manufactured structures (BAMS) are the most preferred functionally graded materials for industrial purposes [2]. These structures have two metallic parts with complementary physical and mechanical properties, such as hardness and corrosion resistance capabilities. Using additive manufacturing techniques to produce bimetallic components is a promising fabrication process to improve industrial components' physical and mechanical properties. These components can be used in many industrial fields with their functional properties in addition to weight-gain and cost reduction, including aerospace, marine, and automotive applications [3-5].

Wire or powder-fed technologies are the two main direct energy deposition (DED) techniques to build homogeneous metallic components of various structural alloys or bimetallic components and some review papers discuss metal additive manufacturing methods including wire arc additive manufacturing (WAAM) [6-7]. Many additively manufactured bimetallic structures have been fabricated via a laser-based powder-fed direct energy deposition process [8-9]. However, WAAM technology is settled in many research centers with low system setup costs, extensive wire-feedstock options, and medium/large-scale

component fabrication capabilities [10-11]. Thus, industrial robot welding technologies with gas metal arc welding (GMAW), gas tungsten arc welding (GTAW), or plasma arc welding (PAW) are utilized to build WAAM-based large-scale components with different wire-feedstock in various industrial applications [12-13]. Moreover,

Nickel and stainless steel-based wire feedstock are widely used for bimetallic structures [14-16]. Among the bimetallic structures, cutting equipment (with wear-resistant cutting edges) related to bimetallic components is one of the significant industrial applications. With their physical and mechanical performance, these bimetallic structures offer cost-effective long-term protection against wear and erosion and hence have longer service life or less repair and maintenance. Hence, the present study explored the feasibility of WAAM technology in manufacturing bimetallic cutting equipment.

2. MATERIAL AND METHOD

To produce a bimetallic cutting equipment, the OTC Daihen FD-B6L manipulator was used as a robot arm with GeKaMaC Power MIG WB 500L synergetic welding machine as a power supply. The integrated robotic WAAM cell consists of the welding robot, welding machine, welding wire, and temperature monitoring systems having a pyrometer and thermal camera. A cleaver is a cutting equipment that needs to have a sharp cutting edge with corrosion resistant body. In addition, this bimetallic structure is expected to provide high hardness values with sufficient ductility. Thus, a bimetallic equipment has been produced using two different filler materials: GeKaTec 600 G (MSG 6 GZ-60 acc. to DIN 8555) hard-facing solid wire and GeKa ELOX SG 316 L Si (ER 316LSi acc. to AWS A5.9) austenitic stainless solid wire. As described in DIN 8555, the MSG 6 group alloy is mainly used in cutting tools, blades of shears, and rolls for cold rolling mills due to its high carbon content leading to high hardness values over 500 HB [17]. The WAAM cell used in this study is shown in Figure 1.

The chemical compositions of the ER 316LSi and MSG 6 GZ-60 are given in Table 1. The S355J2-N low-alloyed steel with dimensions of 350 mm X 150 mm X 12 mm was used as the substrate material. The diameter of all solid wires selected for the experiment is 1.2 mm. The most outstanding feature of the WAAM process is that it can be produced close to near-net shape. Therefore, the robot is programmed according to the cleaver shape. While programming the robot tool paths, the torch was kept perpendicular to the direction of movement (90°) on the deposited part to prevent macro and microstructural defects caused by different heat dissipation. The initial order of the applied wall was changed in each layer at the beginning and end of the deposited wall, as shown in Figure 2.

Figure 1. The robotic WAAM cell used to manufacture bimaterial cleaver

A total of 65 layers were deposited while manufacturing the WAAMed part. A stainless steel wire (ER 316LSi) with 18%wt Cr and 11%wt Ni content was used to deposit first 55 layers. The hard-facing wire was used in depositing the last ten layers on top of the stainless material. The stainless-steel section was processed with the arc current of 110 A with a voltage of 15 V and scanning speed of 40 cm/min, and then the hard-facing wire was directly deposited on top of the ER 316LSi section with a 100 A with the voltage of 18 V and scanning speed of 40 cm/min. The selection of the shielding gas composition has great importance due to the influence on the heat transfer in the welding zone. The gas mixture containing 97.5% Ar + 2.5% CO_2 and 82% Ar + 18% CO_2 mixture of shielding gas atmosphere having a flow rate of 15 $l.min^{-1}$ were used as

shielding gas for austenitic stainless steel and hard-facing wire, respectively.

Table 1. Chemical compositions of the welding wires (wt.%).

	C	Si	Mn	P	S	Ni	Cr	Cu	Mo
ER 316LSi	0.02	0.95	1.80	0.031	0.010	11.18	18.07	0.20	2.01
MSG 6 GZ-60	0.45	2.78	0.37	0.017	0.001	0.10	8.95	0.05	0.01

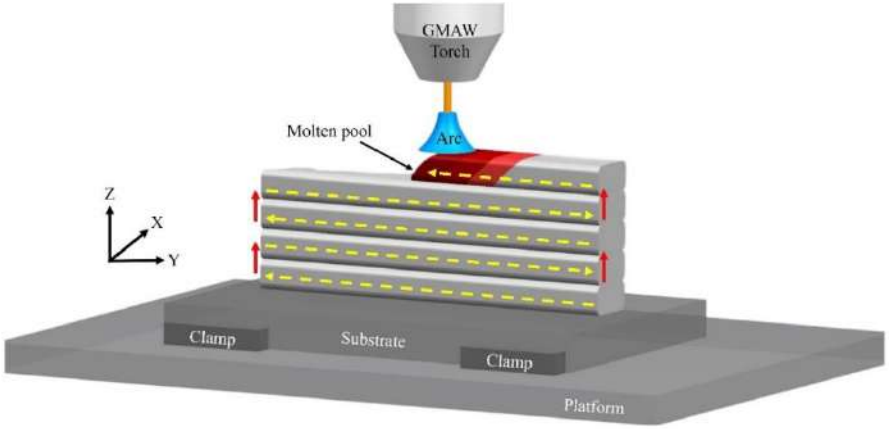

Figure 2. The toolpath orientation used in the study.

Table 2. Process parameters used during the deposition.

Process parameters	Units	ER 316LSi	MSG 6 GZ-60
Current	A	110	100
Voltage	V	15	18
Wire diameter	Mm	1.2	1.2
Moving speed	cm/min	40	40
Torchning angle	Degree	90	90
Shielding gas	-	97.5 Ar + 2.5 % CO2	82 Ar + 18 % CO2
Gas flow rate	l/mm	15	15

As stated in the previous study [14], heat accumulation increases in the WAAM process resulting in local differences in microstructural and mechanical properties, leading to inhomogeneous material properties. Moreover, as the previous layer is preheated, heat can accumulate throughout the building during layer-by-layer production [18]. Wu et al. explained that with the increase of heat accumulation in part produced by the WAAM method, the width of the weld seam also increases due to the changing form of heat transfer during layer-by-layer production [19]. Thus, the WAAMed cleaver was additively manufactured using a dwell time of 120 seconds between each layer to minimize the effect of heat accumulation. The process parameters in the WAAM process are summarized in Table 2.

X-Ray radiographic inspection was performed on the bimetallic component to reveal any indication of the presence of defects between the layers that may have resulted during the deposition process. The Vickers hardness and metallographic samples were taken from the end of the WAAMed cleaver. Standard metallographic methods, including grinding, polishing, and etching, were applied to obtain phase contrast between the layers to hard facing and stainless-steel side, using a 10% NaOH solution and 3% Nital, respectively. The ARL OES 8860 optical emission spectrometer was utilized to perform chemical analyses. The macro and microstructural characterizations along the building direction, including the bimetallic interface, were performed using the Leica DMi8 optical microscope. Finally, Vickers hardness tests were conducted using Struers DuraScan G5 in the transversal section of the WAAMed component.

3. EXPERIMENTAL RESULTS

Bi-material cutting equipment, represented as a cleaver, shown in Figure 3, is manufactured using two different solid wires, AWS ER 316LSi and MSG 6 GZ-60; the latter is a hard-

facing wire to play a role of a cutting edge. The literature research showed that this is the first ever manufactured bi-material cleaver using WAAM technology with two wires.

Figure 3. The general view of bi-material cleaver manufactured using WAAM technology and two different wires: a) as-printed, b) as-machined, c) macro structure of the cross-section of total 65 layers using two different wires.

The macro-section of the deposited layers is also shown in Figure 3, which exhibits rather a successful deposition of a total of 65 layers using stainless steel and hard-facing wires. The macro-section was also used to conduct detailed characterization work of the microstructures and interface area between two materials.

Two different temperature data were collected from the substrate surface and WAAMed cleaver during deposition. These are measured local and full-field temperature data. Figure 4 shows the regional temperature variation measured at a fixed spot of the pyrometer 2 mm away from the substrate during the deposition of the 1st to 20th layers. The temperature curve is composed of a series of peaks showing the development of temperatures in the part. The peak temperatures were higher for the first couple of layers, then decreased gradually with the proceeding layers, and finally kept stayed stable below 200 °C after 15 layers. The increase in layers during deposition causes a change in the heat transfer behavior of the build-up part. In the first layer, the heat is intensely transmitted to the cold substrate via conduction, then transferred to the atmosphere through radiation and via convection with increased layers. Finally, as the number of layers increases, heat transfer (heat loss) to the substrate becomes less, while heat transfer to the atmosphere by radiation and convection becomes more efficacious [20].

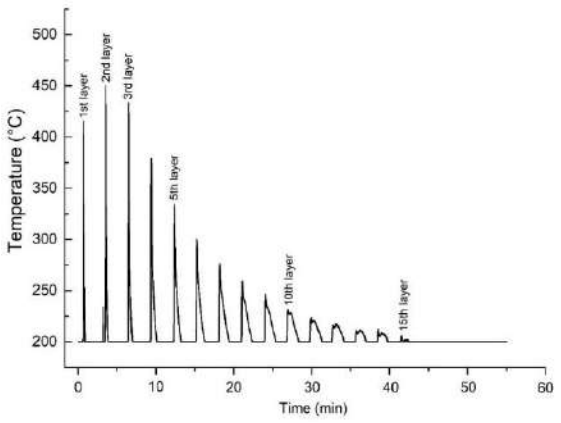

Figure 4. The temperature variation of the substrate during the deposition of first 15 layers, showing that heat transfer to the substrate plate decreases as the numbers of layers increases.

The temperature monitoring of the whole WAAM part was conducted to register the

thermal history of the part during manufacturing, as shown in Figure 5. Knowing the experienced heat cycles and peak temperatures is essential to control the process parameters to obtain homogeneous microstructural development.

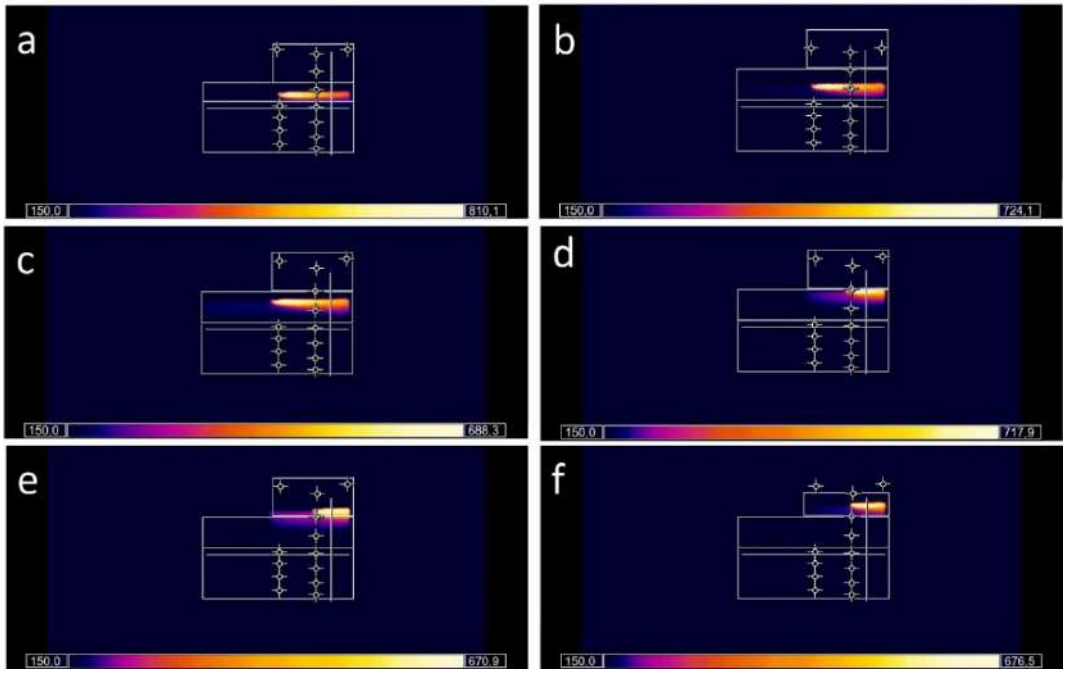

Figure 5. The temperature variation of entire part during the deposition

The elemental mapping obtained from the interface of the bimetallic cleaver is shown in Figure 6.

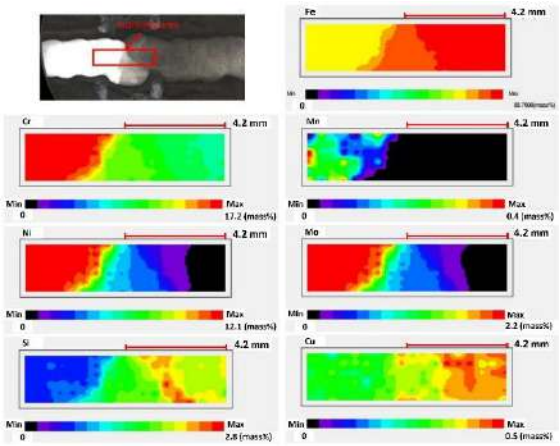

Figure 6. The elemental mapping of interface of bimetallic cleaver.

The results indicate the occurrence of elemental diffusion, resulting in a mixing zone composed of ER 316LSi and MSG 6 GZ-60. The decrease in Cr, Ni, and Mo amounts was observed at the ER 316LSi side of the interface, while the Fe and Cu increased. The mixing zone's width changed with the layers' overlap configuration and was found between 3.5 – 4 mm, indicating considerable dilution between these two materials.

The microstructures in each section were characterized and depicted in Figure 7. The Schaeffler diagram is the most used diagram to estimate the δ-ferrite content in the final microstructure of corrosion-resistant steel with carbon content up to 0.25% after welding [21]. The chromium (Creq) and nickel equivalent (Nieq) were calculated as 21.5 and 12.7, respectively, having a ratio of Creq/Nieq of 1.69. Under the equilibrium state of solidification conditions, this ratio leads to have a ferrite-austenite solidification, in which δ-ferrite is the leading phase, and austenite (γ) is the second phase [22-23]. This is consistent with the experimental findings from Figure 7, where the various δ-ferrites morphologies (dark region), such as skeletal, lathy, etc., occurred in an austenite matrix (light area) at the ER 316LSi side. However, due to the high carbon and chromium content, the top of the bimetallic structure (where the hard-facing wire was used) was characterized as a martensitic matrix with carbides along the grain boundaries. Special attention was given to the characterization of the bi-material interface microstructure since this interface may exhibit local microstructure that may be considered critical for the structural integrity and reliability under the loading of the cutting blade. The investigated interface regions

showed excellent bonding between the two materials. No micro-pores and cracks were found at the interface as shown in Figure 7b and Figure 7d.

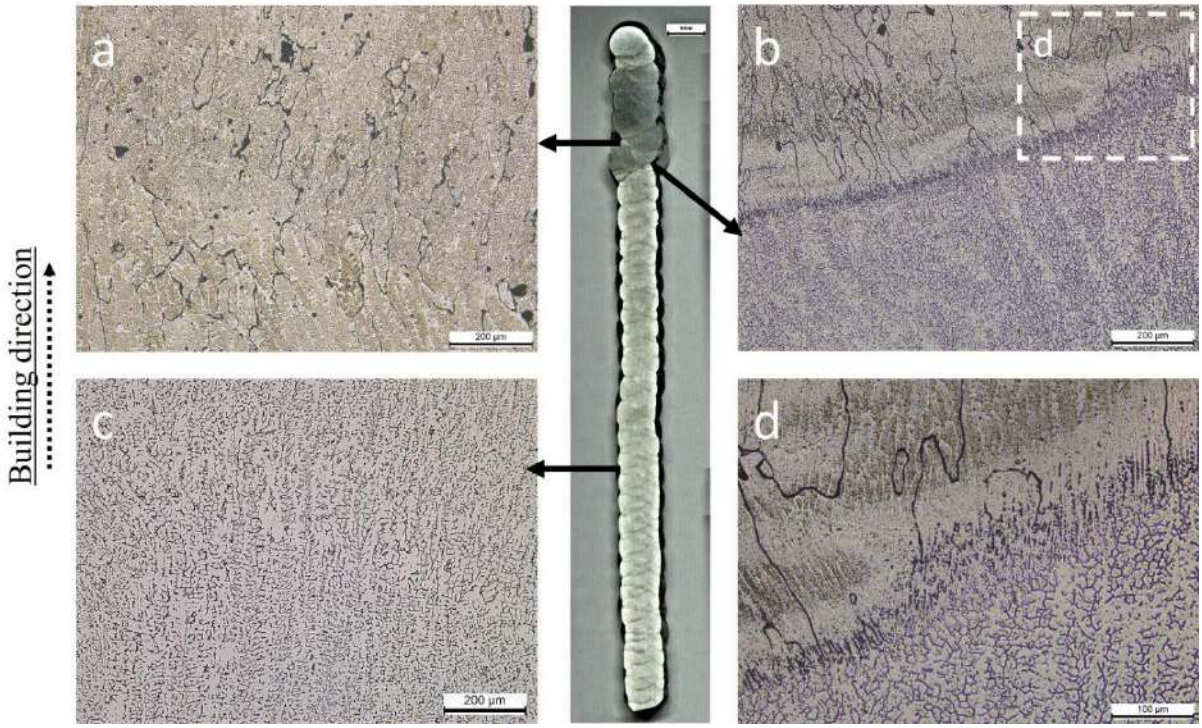

Figure 7. The optical micrographs of the microstructures of the bimetallic cleaver WAAM part show different parts. Note the interfacial region between two materials in two magnifications, Figure 6b and 6d

A hardness testing on all parts of the bimetallic structures is usually performed to evaluate local variations in the materials' properties which may influence the joint's strength and structural performance. Therefore, the Vickers micro-hardness test was carried out to characterize the mismatch between materials and across the interface. The hardness values obtained along the building direction are shown in Figure 8.

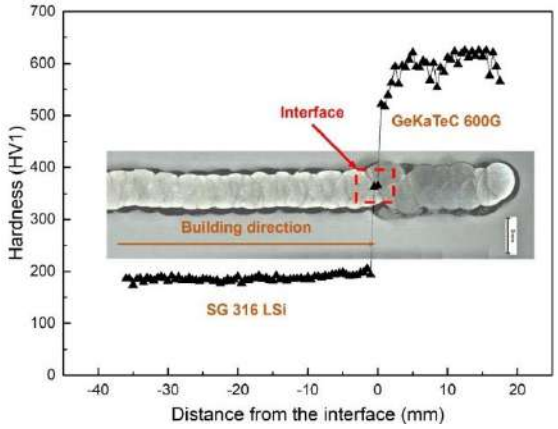

Figure 8. The hardness variation of the bimetallic cleaver (chopping-cleaver) material along the building direction.

The manufacturer specifies the hardness of hard-facing wire as 55-60 HRC, which is also equal to about 596-699 HV [24]. The stainless-steel side of the bimetallic cleaver was measured as 187 ± 5 HV, showing relatively stable hardness results along the build-up direction until the interface, where the hardness increased suddenly, as expected. This sudden increase could be attributed to dilution from the hard-facing side, resulting from elemental segregation (Figure 6). Han et al. [25] also reported similar results for the bimetallic structures manufactured with low alloy steel (ER80S-G) and a hard-facing material (MF6–55GP). Moreover, the average hardness of the hard-facing side started from 2 mm away from the interface and was measured as 600 ± 20 HV. The tempering due to thermal cycling resulted in hardness deviation ranging between 563 HV (as transition region) and 625 HV on the hard-facing side.

The hardness survey of the WAAM material shows that this technology can be used to manufacture hard cutting-edge or zone of high resistance to wear. Furthermore, this means that WAAM can successfully be used for the functionalization of the parts where higher or different structural performance is required from the region.

4. CONCLUSIONS

In this work, a bimetallic component having a total of 65 layers has been additively manufactured to obtain a bimetallic cleaver having high hardness values at the sharp edge. Results showed that a defect-free bi-metallic cleaver with sound microstructure was obtained using WAAM technology, including the interface. As a result, the hardness value gradually increased from the ER 316LSi to MSG 6 GZ-60 and reached over 600 HV. Furthermore, the sharp edges of the bimetallic cleaver were obtained successfully with machining.

This research work demonstrated a new route for manufacturing bimetallic structures and provided more flexibility for designing cutting equipment with site-specific properties for specific structural or functional applications. In the future, special cutting equipment having high corrosion and wear resistance in extreme conditions will also be developed using metal-cored welding wires as a feedstock of the WAAM process instead of solid welding wire to have more design opportunities in arranging the chemical composition with small batches.

ACKNOWLEDGES

This study has been supported by the Scientific and Technological Research Council of Turkey (TUBITAK) under the scope of the University-Industry Cooperation Support Program with project number 5220023. The authors also wish to thank staff members of the Gedik Welding-Türkiye for their technical support during the manufacturing of the WAAM part. In addition, this study has been presented at 6th International Congress on 3D Printing (Additive Manufacturing) Technologies and Digital Industry 2022 between 22-23 Nov. 2022.

REFERENCES

1. Chen, X., Han, J., Wang, J., Cai, Y., Zhang, G., Lu, L., Xin, Y., Tian, Y., “A functionally graded material from TC4 to 316L stainless steel fabricated by double-wire + arc additive manufacturing”, Materials Letters, Vol. 300, Pages 130-141, 2021.

2. Wu, B., Qiu, Z., Pan, Z., Carpenter, K., Wang ,T., Ding, D., Duin, S.V., Li, H., “Enhanced interface strength in steel-nickel bimetallic component fabricated using wire arc additive manufacturing with interweaving deposition strategy”, Journal of Materials Science & Technology, Vol. 52, Pages 226–234, 2020.

3. Ahsan, M.R.U., Fan, X., Seo, G.J., Ji, C., Noakes, M., Nycz, A., Liaw, P.K., Kim, D.B., “Microstructures and mechanical behavior of the bimetallic additively-manufactured structure (BAMS) of austenitic stainless steel and Inconel 625”, Journal of Materials Science & Technology, Vol. 74, Pages 176–188, 2021.

4. Sasikumar, R., Kannan, A.R., Kumar, S.M., Pramod, R., Kumar, N.P., Shanmugam, N.S., Palguna, Y., Sivankalai, S., “Wire arc additive manufacturing of functionally graded material with SS 316L and IN625: Microstructural and mechanical perspectives”, CIRP Journal of Manufacturing Science and Technology, Vol. 38, Pages 230–242, 2022.

5. Ahsan, M.R.U., Tanvir, A.N.M., Ross, T., Elsawy, A., Oh, M.S., Kim, D.B., “Fabrication of bimetallic additively manufactured structure (BAMS) of low carbon steel and 316L austenitic stainless steel with wire arc additive manufacturing”, Rapid Prototyping Journal, Vol. 3, Pages, 519–530, 2020.

6. Çam, G., “Prospects of producing aluminum parts by wire arc additive manufacturing (WAAM)”, Materials Today: Proceedings, Vol. 62, Pages 77-85, 2022

7.

8. Güler, S., Serindağ, H.T., Çam, G., “Wire arc additive manufacturing (WAAM): Recent developments and prospects”, Mühendis ve Makine (Engineer and Machinery), Vol. 63, Pages 82-116, 2022

9. Zhang, C., Chen, F., Huang, Z., Jia, M., Chen, G., Ye, Y., Lin, Y., Liu, W., Chen, B., Shen, Q., Zhang, L., Lavernia, E.J., “Additive manufacturing of functionally graded materials: A review”, Materials Science and Engineering : A, Vol. 764, 138209, 2019.

10. Zhang, W.Q., Zhang, B.P., Xiao, H.F., Zhu, H.H., “Interfacial phenomena and microstructure of copper/steel bimetal structure produced by a new hybrid additive manufacturing process combining selective laser melting and directed energy deposition”, Materials Science Forum, Vol. 1054, Pages 31–36, 2022.

11. Wu, B., Pan, Z., Ding, D., Cuiuri, D., Li, H., Xu, J., Norrish, J., “A review of the wire arc additive manufacturing of metals: properties, defects and quality improvement”, Journal of Manufacturing Processes, Vol. 35, Pages 127-139, 2018.

12. Gürol, U., Dilibal, S., Turgut, B., Koçak, M., "Characterization of a low-alloy steel component produced with wire arc additive manufacturing process using metal-cored wire", Materials Testing, Vol. 64, Issue 6, Pages 755-767, 2022.

13. Chaturvedi, M., Scutelnicu, E., Rusu, C.C., Mistodie, L.R., Mihailescu, D., Subbiah A.V., "Wire arc additive manufacturing: Review on recent fndings and challenges in industrial applications and materials characterization", Metals, Vol. 11, Issue 6, Issue 939, Pages 1-39, 2021.

14. Motwani, A., Kumar, A., Puri, Y., Lautre N.K., "Mechanical characteristics and microstructural investigation of CMT deposited bimetallic SS316LSi-IN625 thin wall for WAAM", Welding in the World, 2022.

15. Gürol, U., Turgut, B., Güleçyüz, N., Dilibal, S., Koçak, M. "Development of multi-material components via robotic wire arc additive manufacturing" International Journal of 3D Printing Technologies and Digital Industry, Vol. 5, Issue 3, Pages 721 – 729, 2021.

16. Jin, W., Zhang, C., Jin, S., Tian, Y., Wellmann, D., Liu, W., "Wire arc additive manufacturing of stainless steels: A review", Applied Sciences, Vol. 10, Issue 5, 1563, 2020.

17. Jafari, D., Vaneker, T.H.J., Gibson, I., "Wire and arc additive manufacturing: Opportunities and challenges to control the quality and accuracy of manufactured parts", Materials & Desing, Vol. 202, 109471, 2021.

18. DIN 8555-1, "Filler metals used for surfacing; filler wires, filler rods, wire electrodes, covered electrodes; designation; technical delivery conditions" November 1983.

19. Wang, J.F., "Effect of location on microstructure and mechanical properties of additive layer manufactured Inconel 625 using gas tungsten arc welding", Materials Science and Engineering A, Vol. 676, Pages 395-405, 2016.

20. Wu, B., Pan, Z., Chen, G., Ding, D., Yuan, L., Cuiuri, D., Li, H., "Mitigation of thermal distortion in wire arc additively manufactured Ti6Al4V part using active interpass cooling", Science and Technology of Welding and Joining, Vol. 24, Issue 5, Pages 484–494, 2019.

21. Jorge, V.L., Teixeira, F.R., Scotti, A., "Pyrometrical interlayer temperature measurement in WAAM of thin wall: strategies, limitations and functionality", Metals, Vol. 12, Issue 765, 1-18, 2022.

22. Bandyopadhyay, A., Zhang, Y., Onuike, B., "Additive manufacturing of bimetallic structures", Virtual and Physical Prototyping, Vol. 17, Issue 2, Pages 256-294, 2022.

23. Saboori, A., Aversa, A., Marchese, G., Biamino, S., Lombardi, M., Fino, P., "Microstructure and mechanical properties of AISI 316L produced by directed energy deposition-based additive manufacturing: A review", Applied Sciences, Vol. 10, Issue 9, 3310, 2020.

24. Rodrigues, T.A., Escobar ,J.D., Shen, J., Duarte, V.R., Ribamar, G.G., Avila, J.A., Maawad, E., Schell, N., Santos, T.G., Oliveira, J.P., "Effect of heat treatments on 316 stainless steel parts fabricated by wire and arc additive manufacturing: Microstructure and synchrotron X-ray diffraction analysis", Additive Manufacturing, Vol. 48, Part B, 102428, 2021.

25. Hardfacing Welding Wires And Rods, "600G", https://gedikwelding.com/en/product-detail/600-g, October 27, 2022.

26. Han, S., Zhang, Z., Liu, Z., Zhang, H., Xue, D., "Investigation of the microstructure and mechanical performance of bimetal components fabricated using CMT-based wire arc additive manufacturing", Materials Research Express, Vol. 7, 116525, 2020.